

# Real-World Impact of Robotic-Assisted Bronchoscopy on the Staging and Diagnosis of Lung Cancer: The Shape of Current and Potential Opportunities

Gabriel Ortiz-Jaimes<sup>1,\*</sup>, Janani Reisenauer<sup>1,2,\*</sup>

<sup>1</sup>Division of Pulmonary and Critical Care Medicine, Mayo Clinic, Rochester, MN, USA; <sup>2</sup>Division of Thoracic Surgery, Mayo Clinic, Rochester, MN, USA

\*These authors contributed equally to this work

Correspondence: Janani Reisenauer, Division of Pulmonary and Critical Care Medicine, Division of Thoracic Surgery, Mayo Clinic, 200 1st St, SW, Rochester, MN, 55905, USA, Email [reisenauer.janani@mayo.edu](mailto:reisenauer.janani@mayo.edu)

**Abstract:** The approach to peripheral pulmonary lesions (PPL) has been evolving continuously. Advanced bronchoscopic navigational techniques have improved the airway-based approaches to these lesions. Robotic Assisted Bronchoscopy (RAB) can be considered the current pinnacle of this evolution; allowing for a safer approach to sampling lesions previously considered outside of bronchoscopic reach. We present a comprehensive review of the changing epidemiology of lung cancer and the importance of early tissue sampling, the evolution of sampling and navigational bronchoscopic techniques, technical considerations and evidence pertaining to the use of RAB, and adjunct techniques in the diagnosis of lung cancer. Complications and future applications of RAB are also discussed.

**Keywords:** lung cancer, navigational bronchoscopy, pulmonary nodule, robotic bronchoscopy

## Epidemiologic Considerations

Lung cancer continues to be the leading cause of cancer-associated death worldwide.<sup>1</sup> Recent developments in screening, diagnosis, and treatment, along with decades of efforts to reduce tobacco use, have been fruitful in improving outcomes. In 2022, 236,740 new cases were diagnosed, and 130,180 lives were lost due to lung cancer in the US, representing an improvement from 160,340 deaths in 2016. This improvement in lung cancer mortality has been the major factor in reducing overall cancer mortality; statistics show a decrease in lung cancer death rate of 56% in men (1990–2019) and 32% in women (2002–2019).<sup>2</sup> Nonetheless, it is estimated that yearly there will be 1.8 million new lung cancer cases diagnosed and 1.6 million deaths worldwide, more than those caused by tuberculosis, malaria, and HIV.

There is a direct correlation between the stage at diagnosis and mortality, which has shaped the staging systems over time. The challenge of early diagnosis continues to be one of the most pertinent, as lung cancer continues to be diagnosed at an advanced stage up to 74% of the time, with metastatic disease present in 46% of cases.<sup>3</sup> While 5-year survival for prostate, breast, and colorectal cancer approaches >95%, 90%, and 65%, respectively, Stage I lung cancer is not entirely comparable to these malignancies ranging from 58–73%. In comparison, overall 5-year survival for all stages is 23.7%, and 7% for advanced distant disease alone.<sup>3</sup>

While survival is heterogeneous by lung cancer type, the recent decline in the mortality rate for non-small cell lung cancer (NSCLC) suggests that advances in diagnosis and treatment have been impactful in improving cancer-specific survival. On the other hand, small cell lung cancer (SCLC) associated mortality has declined almost exclusively due to a decline in incidence with no improvements in cancer-specific survival, reflecting less significant advances in treatment.<sup>4</sup>

Therefore, developing techniques that allow for a more precise diagnosis at earlier stages is of paramount relevance. Robotic-assisted navigational bronchoscopy (RAB) has been one of these major advancements in diagnosis and continues to demonstrate potential for ongoing novel developments in diagnosis and treatment.

## Lung Cancer Screening and the Need for Earlier and More Precise Diagnostic Strategies

The significant decrease in cancer-specific mortality since 2013 has coincided with two important changes in the approach to lung cancer, the first being the recommendation for lung cancer screening in 2014.<sup>4</sup> After the failure of periodic chest X-rays in lung cancer screening in the Prostate, Lung, Colorectal, and Ovarian cancer screening (PLCO) trial,<sup>5</sup> 2 major studies with low-dose chest CT (LDCT) scans have changed the practice in recent years.

The National Lung Screening (NLST) trial demonstrated a higher detection of benign and malignant lesions in 53,454 high-risk individuals, with an odds ratio for cancer diagnosis of 1.13 in the LDCT-screened group compared to chest radiographs. Detection, diagnosis, and treatment of these cancers led to significant decreases in relative lung cancer-specific mortality of 20% and all-cause mortality of 6.7%.<sup>6</sup> The European-based NELSON trial, utilizing a different interval LDCT schedule with volumetric analysis in 15,789 high-risk individuals, demonstrated a cancer-specific mortality benefit in the screening group (OR 0.76) for up to 10 years of follow-up.<sup>7</sup>

In the NELSON trial, the most common stage of cancer at diagnosis was IA (46%) in the screening group vs stage IV (45%) in the un-screened population. Similarly, in the NLST, 40% of the cancers diagnosed in the screened arm were stage IA vs 11% IIIB and 21% IV, whereas, in the x-ray arm, 36% were diagnosed in stage IV (the most common stage at diagnosis) and only 21% in Stage Ia.

Based upon the NELSON trial, the United States Preventive Services Taskforce recommends screening for lung cancer based on a 20-pack per year history instead of 30. This will lead to the screening of approximately 14.5 million individuals, an increment of 6.5 million people compared to previous screening parameters. Subsequently, this will result in 40,000 diagnoses of early lung cancers per year.<sup>8</sup> This epidemiological trend of increased proportions of early-stage disease will continue to generate the need for tissue sampling in smaller lesions which may be more challenging to differentiate from benign lesions pre-biopsy. As the likelihood of cancer decreases when sampling smaller lesions, a higher degree of precision is necessary, particularly in the case of PPL.

## The Importance of Early Tissue Sampling for Molecular Markers

The second significant event thought to have decreased lung cancer mortality was the recommendation for epidermal growth factor receptor (EGFR) and anaplastic lymphoma kinase (ALK) mutation testing in adenocarcinoma lesions, and the FDA approval of targeted therapies, such as EGFR inhibitors as first-line therapies in 2013.<sup>1,4</sup> The identification of mutations, particularly of the EGFR gene, or rearrangements in the ALK gene and the c-ROS-1 oncogene, has been shown to have prognostic implications.<sup>9</sup> Along with the above, programmed cell death ligand (PD-L1) expression levels have also demonstrated the ability to predict response to therapies targeted at these anomalies, significantly improving clinical outcomes, including mortality.<sup>10</sup> Current guidelines recommend testing of all lesions containing any component of adenocarcinoma or in patients who have no or minimal smoking history. Testing for at least these three driver mutations should be carried out in samples with acceptable cellularity of at least 20% or more malignant cells.<sup>11</sup>

Mediastinal and hilar curvilinear endobronchial ultrasound (C-EBUS) transbronchial needle aspiration (TBNA) samples obtained during the staging of suspicious or known malignant lesions are frequently adequate for molecular analysis in a meta-analysis including 28 studies with 2698 patients, 94.5% of the samples were suitable for EGFR and 94.9% for ALK mutation detection.<sup>12</sup> Previously, the treatment of node-negative early peripheral lesions relied on molecular analysis of surgical pathology after resection, frequently having to proceed with primary surgical diagnosis and resection in the same procedure. Patients with targetable mutations can now benefit from the recent approval of adjuvant targeted therapy and immunotherapy in addition to standard chemotherapy after resection.

The CheckMate 816 trial included 682 patients with stage IB to IIIA resectable NSCLC and found that neoadjuvant chemoimmunotherapy, including the fully human anti-PD-1 antibody nivolumab as conjunction immunotherapy led to

a longer and significant improvement in event-free survival of 31.6 vs 20.8 months when compared with neoadjuvant chemotherapy alone (hazard ratio for death, progression, or recurrence 0.63 95% CI 0.43–0.91  $p$  0.005). The intervention arm was associated with a higher likelihood of having no viable tumoral tissue on resected specimens (24% vs 2.2%, odds ratio 13.94). Thirty-five percent of these patients were randomized at stage IB or II, and the surgical resection cancellation rates due to disease progression were under 10%. Notably, the 7th edition staging system was used, making most of the IB lesions a stage IIA under the current 8th edition. The PD-1 expression level by immunohistochemistry was a significant predictor of success in the nivolumab arm, with expression levels <1% not correlating with a beneficial effect (HR 0.85 95% CI 0.54–1.32) and expression >50% strongly correlating with significant event-free survival (HR 0.24 95% CI 0.1–0.61). Given concerns with mutual exclusion for simultaneous therapy in patients with EGFR and ALK mutations, and the potential differentiating role of PD-L1 expression levels, all patients required sufficient tissue for molecular analysis long before their surgical resections.<sup>13</sup> Similarly, the KEYNOTE-671 trial<sup>14</sup> demonstrated positive findings when utilizing neoadjuvant pembrolizumab in 797 patients as early as Stage II (29.7% in the treatment arm), 37% of the patients had N0 nodal status, thus, relying only on biopsies of the primary site. Improved event-free (local progression, unresectable tumor, progression or recurrence, or death) survival (62.4% vs 40.6%,  $p$ <0.001) and overall survival (80.9% vs 77.6%  $p$ =0.02) at 24 months were found. The PD-L1 status significantly impacted the hazard ratio for death (non-significant in <1% and more significant in >50% vs 1–49%). PD-L1 expression testing cannot be performed on liquid biopsy samples.

In the NELSON and NSLT studies, smaller primary lesions and node-negative cancer stages represented most of the cases detected via screening, stage I accounting for 40.4–50% in the screened populations, as opposed to 13.5–31.1% in the un-screened groups. The growing role of neoadjuvant chemoimmunotherapy, even in early-stage lung cancer, calls for a more aggressive approach to tissue sampling of primary lesions; obtaining appropriate samples for molecular analysis will become paramount when nodal disease is absent. These scenarios, in particular stages IB and non-surgical, node-negative stages II and IIIA, are situations in which guided and robotic bronchoscopy techniques can significantly contribute.

## Traditional Tissue Sampling Techniques: CT Guided Transthoracic Needle Biopsy (CT-TTNB)

CT-TTNB has been the most traditional way to biopsy PPL non-surgically. The diagnostic yield (DY) depends on factors such as nodule size and characteristics, cancer prevalence, and number of needle passes. Sensitivity for cancer is greater than 90% with wide variation (65–94%) with a specificity close to 100% (96–100%). Non diagnostic results occur with a median frequency of 20.5%, however, they are five times more frequent in nonmalignant cases (44% vs 8%).<sup>15</sup>

CT-TTNB is, however, a procedure with a significant risk of complications. A database review of 15,865 TTNB reported an incidence of bleeding of 1%, with 17.8% of them requiring transfusions. The most common and relevant complication is pneumothorax; this series reported an incidence of 15% (95% CI 14–16%), with 6.6% (95% CI 6–7.2%) of all biopsies requiring a chest drain, leading to significant increases in length of stay and respiratory failure.<sup>16</sup> A meta-analysis of 23,104 patients reports a higher rate of pneumothorax of 25.9%, with a similar rate of chest tube placement of 6.9%. Lesion-specific risk factors for pneumothorax included: size smaller than 4 cm (OR 2.09), no pleural contact (OR 1.73), and deeper location (>3 cm, OR 2.38);<sup>17</sup> features that could be more approachable with precise endobronchial techniques.

## Standard and Non-Robotically Guided Bronchoscopic Techniques

Multiple approaches have been developed to attempt tissue sampling of PPL utilizing bronchoscopy; however, incorporating new technology has not always translated into improvements in DY.

Using a probable anatomical location with white light bronchoscopy and 2D fluoroscopy has limited value in evaluating PPL. A systematic review of 35 studies with 4507 patients found an initial sensitivity of 88% in central lesions. In PPL, the yield was significantly lower; when combined with fluoroscopy, 34 studies with 5742 patients

demonstrated an overall sensitivity of 78%; however, when discriminated by size, the yield for lesions <2cm was only 34%.<sup>18</sup> In a multicenter randomized trial of 221 patients in 5 sites, this approach had only a 37% DY.<sup>19</sup>

The development of image-based airway maps, with subsequent intraprocedural tracking of the real-time position of certain bronchoscopic elements, led to the creation of electromagnetic navigational bronchoscopy (ENB/EMN), which received approval for use in the US in 2004.<sup>20</sup> ENB and its combination with imaging modalities have increased the yield of bronchoscopic sampling of PPL.<sup>15</sup> Currently available non-robotic technologies include ENB and virtual bronchoscopy (VB), which can be combined with R-EBUS with or without a guiding sheath. VB and R-EBUS can also be used with thin (4 mm) or ultrathin (3mm) bronchoscopes to allow maneuverability in distal airways. However, these have not demonstrated a significant increase in diagnostic performance.<sup>19</sup> The presence of bronchus sign has been one of the most critical factors in biopsy success using these techniques (OR 2.09), only surpassed by the adjunct of a radial EBUS (REBUS) positive signal (OR 8.56). However, historical cohorts have demonstrated a decrease in the prevalence of the bronchus sign,<sup>21</sup> reflecting potentially smaller and more challenging lesions being considered for bronchoscopic biopsy and a prior intrinsic selection bias.

ENB uses CT images to reconstruct the tracheobronchial tree and plan a pathway to the target lesion. The patient is located within an electromagnetic field, and different sensors can track the bronchoscope position in real-time. The two most utilized manual ENB systems are the SuperDimension (Medtronic, Minneapolis, MN) and the SPiNDrive (Veran Medical Technologies, St Louis, MO). The former uses a sensor loaded into a steerable extended working channel passed through a therapeutic bronchoscope and generates a navigational pathway based on a preprocedural inspiratory CT. The patient lies over a magnetic board, and a predetermined algorithm estimates their respiratory movement. The locatable sensor is removed when biopsy tools are advanced through the channel (Figure 1). The SPiNDrive system requires inspiratory and expiratory CT images and adjusts for respiratory motion using fiducial pads on the patient's chest; the navigational sensor is located at the tip of special bronchoscopes, which allows for continued tracking of position during the sampling phase.<sup>20</sup>

NAVIGATE was a multicenter, single-arm study utilizing the SuperDimension system and the largest ENB study to date, including 1338 patients, and using R-EBUS in 50.6% of the cases. The DY was 67.8%, and sensitivity for malignancy was 62.6%, with close to 50% of the lesions being < 2 cm. The system was also utilized to mark lesions with fiducial markers and dye.<sup>22</sup>

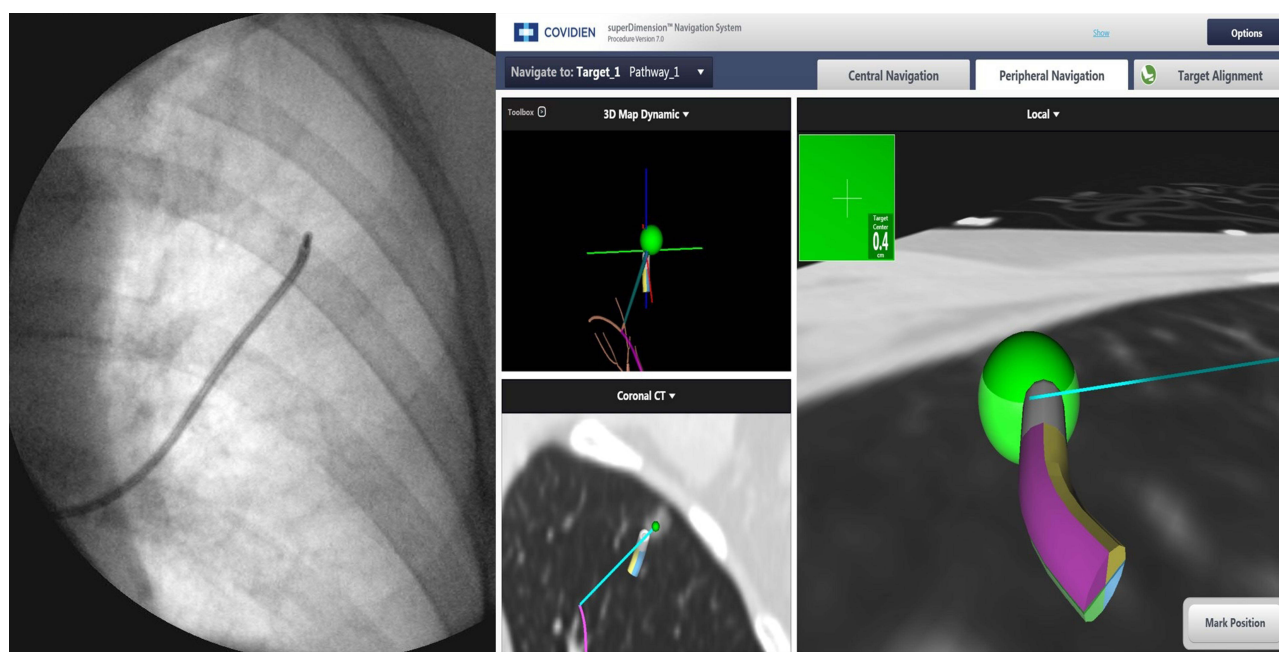


**Figure 1** SuperDimension ENB (Medtronic, Minneapolis, MN) utilized for biopsy and dye marking of a left upper lobe lesion. (Courtesy of Dr. Ryan Kern, Mayo Clinic, Rochester, MN).

Wang et al conducted a meta-analysis of 39 studies and 3052 lesions evaluating the performance of guided bronchoscopy techniques, including ENB, VB, Ultrathin bronchoscopy, R-EBUS, and a guiding sheath. The pooled DY of all methods was 70%. Although there was significant variability among studies, only VB (72%) and R-EBUS (71.1%) had a higher than overall yield, surprisingly higher than ENB (67%). The weighted DY was higher in lesions >20 mm (82.5%) vs <20 mm (60.9%). This demonstrated a significant improvement in PPL sampling compared to standard bronchoscopy with fluoroscopy.<sup>23</sup> An updated analysis of this work in 2023 showed similar findings (discussed later).<sup>24</sup> Folch et al meta-analyzed 40 studies (including NAVIGATE) with 3,342 patients and found a higher DY for ENB of 77% (95% CI 72–82%) with an area under the ROC curve of 0.95 and adequate sampling for ancillary testing in 90% of the cases, 38 studies used the SuperDimension system, and the average lesion size was 23.2 mm.<sup>25</sup> This could represent an improvement in technical implementation, as ROSE, R-EBUS, or fluoroscopy did not perform better.

Additional techniques are in development to improve the yield of EMN bronchoscopy. For example, in a recent direct retrospective comparison with RAB, the use of digital tomosynthesis imaging with the SuperDimension system increased the DY to similar levels reached with SS-RAB when done without cone beam CT (CBCT) guidance (80% vs 77%).<sup>26</sup> The 2013 lung cancer diagnosis guidelines provide a grade IC recommendation to proceed with ENB if expertise and technologies are available.<sup>18</sup>

## Robotically Assisted Bronchoscopy (RAB): Available Technologies

In 2018 and 2019, the Food and Drug Administration (FDA) approved two platforms via a 510 (K) based on “substantial equivalence” between RAB and ENB.<sup>27</sup> These have undergone substantial clinical testing in multiple environments (Table 1).

The Monarch robotic system (Auris Health Inc, Redwood City, CA) utilizes EMN technology via an electromagnetic field generator and reference sensors in the patient’s thorax to determine the position of the target lesion; the catheter is associated with an electromagnetic signal, and the system’s computer adjusts the position, angulation, and distance to

**Table 1** Characteristics of Commercially-Available Robotic Platforms

	<b>Ion Robotic Bronchoscopy System</b>	<b>Monarch Robotic Bronchoscopy System</b>	<b>Galaxy System</b>
Technology Type	Shape-sensing	Electromagnetic Navigation	Electromagnetic Navigation
Catheter Diameter	3.5 mm	Mother- Daughter configuration, 4.2mm Inner extension, 6mm outer catheter	4.0 mm (disposable catheter)
Working Channel	2 mm	2.1 mm	2.1 mm
Maneuverability/flexion	180 °	Outer catheter: 130° Inner catheter 180°	N/A
Endobronchial vision during Navigation	Yes, 1.8 mm vision probe (90–120 degrees field of view)	Yes	Yes
Endobronchial vision during Biopsy	No	Yes	Yes
Controller interface	Console pedestal with secondary screen. Trackball and scroll wheel controller	Video game-like handheld controller	Video game-like handheld controller
Imaging features	Cone Beam CT integration Augmented fluoroscopy under investigation	Cone Beam CT Digital tomosynthesis under investigation	Digital tomosynthesis – augmented fluoroscopy proprietary system. TiLT™ (tool-in lesion technology)

**Notes:** Modified with permission from Duke JD, Reisenauer J. Review: Technology and Techniques for Robotic-assisted Bronchoscopy. *Journal of Lung Health and Diseases*. 2022;6(1):1–5.<sup>28</sup>



target variability with respiration. Pre-procedural CT scans with a recommended slice thickness of 1–1.25 mm and intervals of 0.8–1 mm are used to create an airway pathway. The bronchoscope has a mother-daughter telescopic design with an outer 6 mm catheter with 130° angulation capabilities and an inner 4.2 mm with 180° flexion that can be extended further into distal areas. There is a 2.1 mm working channel, and the catheter has an incorporated video transmission system allowing for an “always on” frontal white light view during the biopsy. Monarch is the EMN-based robotic bronchoscopy (EMN-RAB) prototype<sup>28–30</sup> (Figure 2).

The Ion Endoluminal System (Intuitive Surgical, Sunnyvale, CA) utilizes a novel shape sensing technique (ssRAB) that allows for real-time location of a 3.5mm bronchoscopic catheter based on its deformation while navigating the airways. It utilizes the proprietary PlanPoint planning software, requiring a CT scan with a slice thickness of 0.5–1mm at an interval of 0.5–0.8mm, from which it creates a 3D airway map with target selection and pathway creation options. The catheter is driven via a pedestal-type controller with two controlling mechanisms: a rolling wheel and a trackball to control the advancement, withdrawal, and flexion of the catheter, respectively (Figure 3). The catheter has a flexion of 180° with a 2mm working channel, which can house a 1.8mm vision probe with a visual field of 120°; this probe needs to be removed to allow insertion of biopsy instruments. The company produces proprietary TBNA needles (Flexision) in 19, 21, and 23-gauges.<sup>28,31</sup>

The Galaxy system (Noah Medical, San Carlos, CA) has recently received FDA 510k clearance. Although EMN-based, its main advantage is the incorporation of digital tomosynthesis-based augmented fluoroscopy with real time target position update, designed to address the possible shortcomings of EMN and CT to body divergence (TiLT+: Tool-in-lesion Technology™). It utilizes standard fluoroscopy to generate a 3D reconstruction and a simulated target. Preclinical testing in animal models (MATCH study) with an average pigmented nodule size of 16 mm found 100% success of



**Figure 2** Monarch Robotic System (Auris Health Inc, Redwood City, CA).



**Figure 3** Ion Endoluminal System (Intuitive Surgical, Sunnyvale, CA).

**Notes:** Reproduced with permission from Duke JD, Reisenauer J. Review: Technology and Techniques for Robotic-assisted Bronchoscopy. *Journal of Lung Health and Diseases*. 2022;6(1):1–5.<sup>28</sup>

navigation, with a final Tool-in-lesion (TIL) rate of 95% and pigment present in 100% of the samples.<sup>32</sup> It also offers vision during biopsy and a disposable single-use bronchoscopic catheter.<sup>29</sup> Further human clinical data is not currently available.

## Pre-Procedural Planning

Based on pre-procedural CT scans, different platforms are used to generate navigational airway pathways to reach the target lesion. These tools create a virtual bronchoscopy-based 3D airway map, of which a key factor is the ability to generate as many airway generations as required to reach the lesion and to provide the best transbronchial point of parenchymal entry. The user can highlight the target lesion, select and edit the pathways, and add potential airways not depicted by the automatic rendering process. Occasionally, successful pathways can be created by adding “occult airways” to maps based on the course of vascular structures (“vessel sign”).<sup>33,34</sup> In the largest study by our group, navigation through an average of 7 airway generations was accomplished.<sup>35</sup> The planned pathways and data are then transferred to the robotic console.

The ATLAS Study<sup>36</sup> compared the final distance to target in 41 PPL among automatic pathways generated by three different planning systems: PlanPoint v1.1.0 (used by the ion ssRAB platform), SPiN Planning v4.2.0 (utilized by SPiNDrive ENB) and the SuperDimension ENB system v7.1; 73% of the lesions were located in the outer third of the thorax. Despite all systems being able to similarly generate an average of 3.3 segmental airway generations ( $p$  0.19), the PlanPoint platform used in RAB was superior to the ENB-based systems, with an average distance-to-target of  $9.4 \pm$

5.7mm (compared to  $14.2 \pm 12.9$  and  $17.2 \pm 15.6$ mm achieved by the other systems respectively,  $p < 0.01$ ). This exemplifies why pathway generation is highly heterogeneous and not only dependent on the ability to map and render more distal airways but also on the efficiency of the navigational plans. This adds a layer of complexity to adequate navigation and highlights the importance of imaging confirmation strategies.

## Procedural Considerations

Although procedural steps are highly variable, general principles are frequently followed.<sup>28,30,31,37,38</sup> The patient undergoes general anesthesia, most commonly with total intravenous anesthesia, a large endotracheal tube, and commonly neuromuscular blockade, to guarantee appropriate apneic pauses and prevent inadvertent motion of the target and tools. Anesthetic techniques to decrease CT-to-body divergence will be discussed separately. In our practice, the location of the lesion can dictate the level of PEEP utilized; most commonly, values close to 10 are used for upper lobe lesions and closer to 15 for the lower lobes. The use of tidal volumes close to 10 mL/kg of ideal body weight is frequent. However, the VESPA (Ventilatory Strategy to Prevent Atelectasis) trial demonstrated that a formal ventilatory strategy utilizing a recruitment maneuver, reducing the FiO<sub>2</sub> and having PEEP levels of at least 8 cmH<sub>2</sub>O was effective, and tidal volumes used in this study were lower.<sup>39</sup> At this point, it is essential to ensure that the lesion is centered in the fluoroscopic field of view in all axes to avoid the need for any additional bed movements during navigation.<sup>40</sup>

The robotic catheter is inserted, and a live registration is performed to locate airway landmarks and calibrate the position of the catheter. Simultaneous and coordinated virtual and endobronchial views are offered to allow for ease of navigation (Figures 4 and 5). Discrepancies can present between the plan and the endobronchial views. Navigation can differ between platforms; Monarch offers the possibility of utilizing the outer catheter to splint the more proximal airways. Ion offers a virtual 3D airway map that demonstrates the position of the catheter, the lesion, and the pleural margins, allowing for manipulations when the endobronchial view is suboptimal; it also allows for previewing further steps in the virtual pathway, which can be helpful when the alignment with the endobronchial view is not exact. To prevent tissue injury from forceful advancement in the absence of tactile feedback, Monarch provides buckling errors, and Ion provides continuous measurements of driving force and tip articulation radius. If navigation proves difficult due

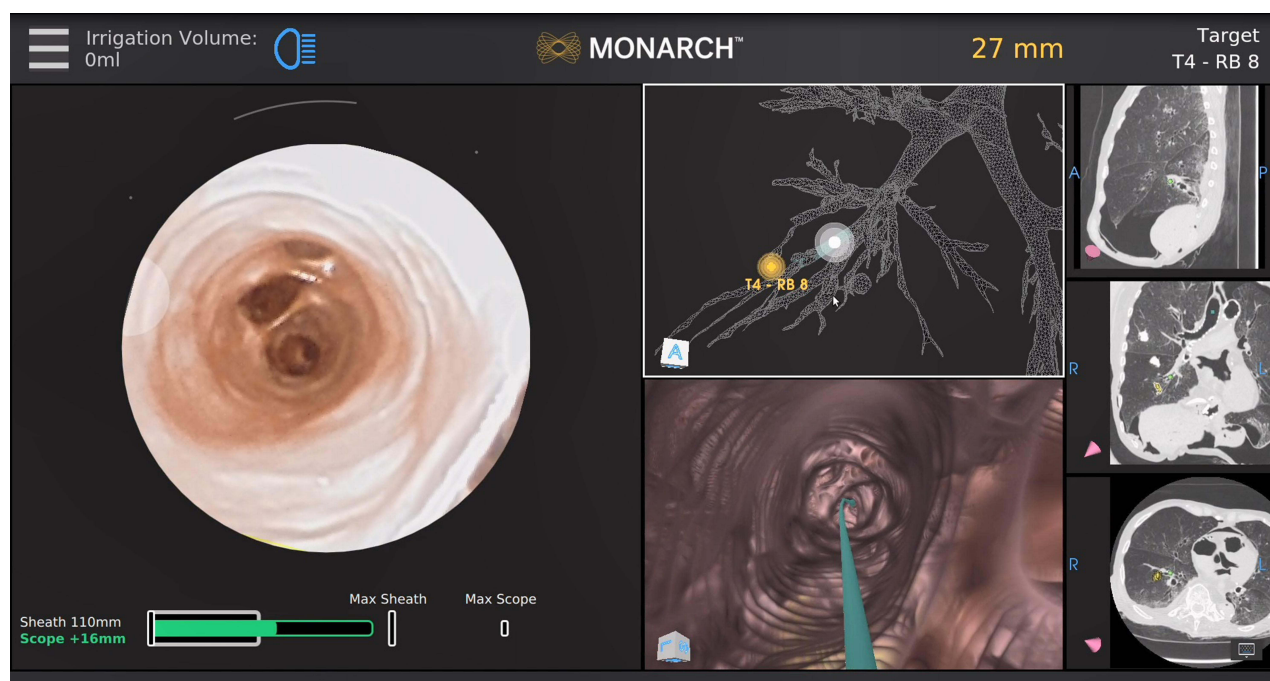


**Figure 4** Monarch system interface displaying endobronchial, virtual bronchoscopic views, navigational pathway, preprocedural CT, and distance to target.

**Notes:** Reproduced with permission from Duke JD, Reisenauer J. Review: Technology and Techniques for Robotic-assisted Bronchoscopy. *Journal of Lung Health and Diseases*. 2022;6(1):1–5.<sup>28</sup>



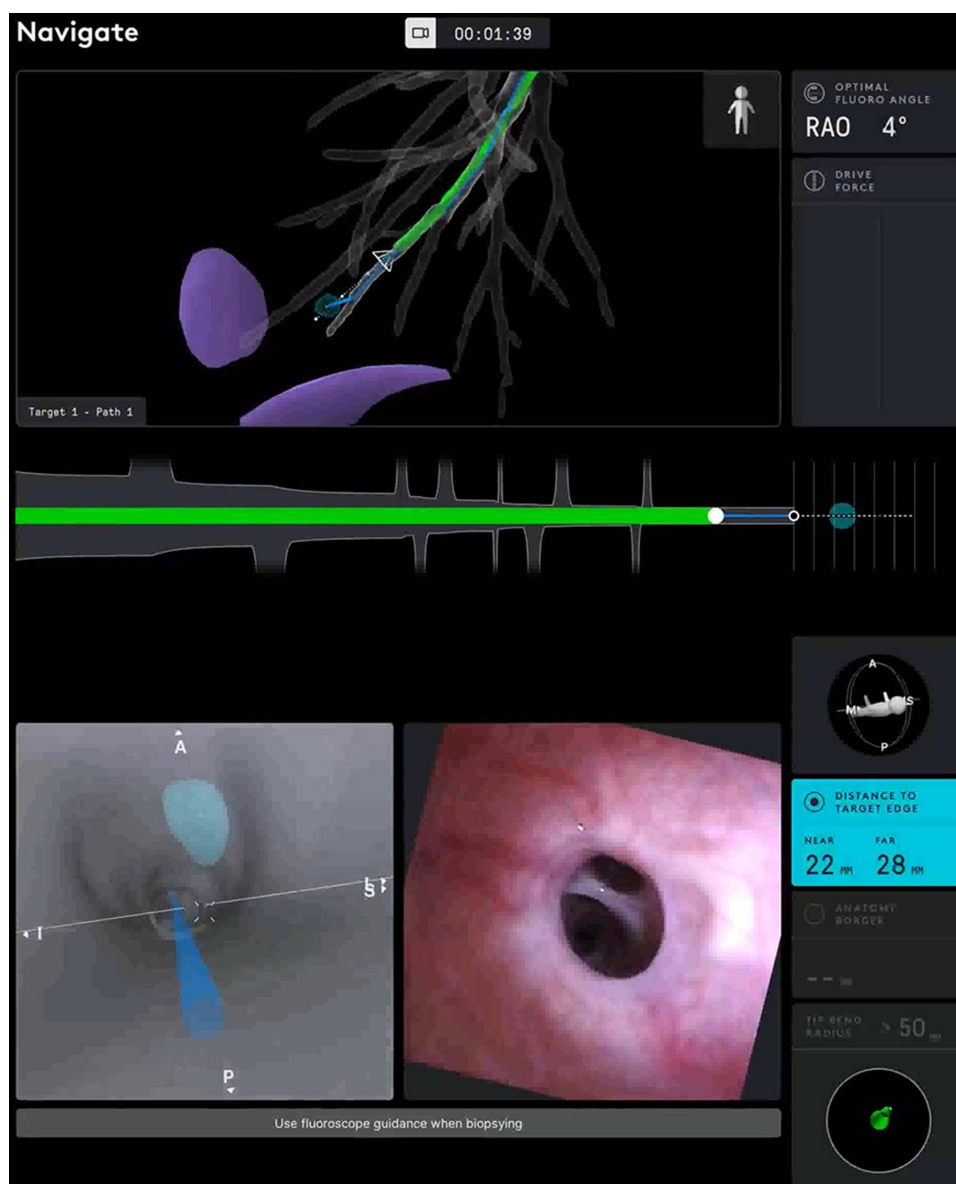


**Figure 5** Ion system interface displaying endobronchial, virtual bronchoscopic views, navigational pathway, pleural margins, and distance to target.

**Notes:** Reproduced with permission from Duke JD, Reisenauer J. Review: Technology and Techniques for Robotic-assisted Bronchoscopy. *Journal of Lung Health and Diseases*. 2022;6(1):1–5.<sup>28</sup>

to the collapse of the airway, insufflation of air through the working channel has been reported.<sup>30</sup> In the largest study, a second navigation pathway had to be attempted in 16% of the cases, and 86% of the nodules were extrinsic to the airways.<sup>35,40</sup>

If a lesion without an endobronchial component is sampled, once the closest airway is reached, an initial assessment with confirmatory tools can be made before biopsying (R-EBUS, CBCT). Occasionally, re-registration of the target position and minor articulations of the catheter position are required. It is essential to ensure that the catheter tip is abutting and indenting the airway wall before sampling, guaranteeing adequate parenchymal penetration and preventing the biopsy instruments from gliding along the airway walls without reaching the lesion.

All studies have utilized an aspirating transbronchial needle as a biopsy tool, as it can be the best initial tool to pierce through the airway wall when there is no endobronchial component. At this point, confirmatory imaging is used to ensure a tool-in-lesion (TIL) position. Needle biopsies are generally performed using aspiration, but the exclusive use of

capillary action with the stylet has been described. At this point, other biopsy tools can be utilized; the number of needle and/or biopsy passes is primarily influenced by Rapid On-Site Evaluation (ROSE) results and clinical suspicion.

## Clinical Evidence in Robotic Bronchoscopy

Since multiple diagnostic possibilities exist (benign, malignant, and non-diagnostic), the most reported metric in RAB literature is the overall diagnostic yield (DY). One of the most commonly used definitions includes a summation of the true positive and true negative results, utilizing the entire clinical picture and evolution of the lesion and/or radiographic and clinical outcomes after follow-up.<sup>22</sup> There is marked heterogeneity in the literature even when this is considered one of the main outcomes.<sup>41</sup> A recent effort to standardize DY has subdivided it into: Strict: a malignant or specific benign diagnosis (granulomatous inflammation) can be made definitively at the time of the procedure; all others are considered non-diagnostic. Intermediate: non-specific benign results (non-specific inflammation) are considered diagnostic if confirmed upon follow-up. Liberal: Non-diagnostic samples (normal tissue) are considered diagnostic if confirmed non-malignant after follow-up.<sup>42</sup>

A remarkably high specificity for positive malignant results is common to all studies; this contrasts with variable proportions of benign and non-diagnostic results, which affect the DY and sensitivity. Procedural adjuncts such as R-EBUS and confirmatory images have an essential impact on DY and have been variably utilized in different studies.

After initial experiences with cadaver and simulated models,<sup>43</sup> clinical studies utilizing both platforms have reported varying DY rates and sensitivities for malignancy. Table 2 summarizes the studies available on RAB in PPL. DY has been reported between 69.1%<sup>44</sup> and 96%.<sup>37</sup> Heterogeneity is widely present in terms of procedural technique, including various forms of imaging and adjunct tools for visualization. The prevalence of malignancy and the pretest probability for a specific malignant or benign diagnosis will unavoidably affect the DY of the procedure. It also influences how persistent the procedural team might be in terms of biopsy attempts or instruments utilized. Reported prevalences of malignancy, when followed longitudinally or when considered in conjunction with other diagnostic techniques, oscillates between 54.5% and 88%. Prospective and retrospective data is available, and some studies have followed patients up to 12 months after the procedure, mainly to corroborate the validity of results based on clinical progression. No direct comparison is available between platforms thus far.

As with other techniques, Chadda found that the most significant predictors of a successful and diagnostic biopsy were the presence of a bronchus sign (OR 2.3 95% CI 1–5.3 p 0.04) and the R-EBUS signal, with a concentric signal being the most robust predictor (OR 10.0 95% CI 3.2–31.1 p <0.001) followed by an eccentric signal (OR 7.4 95% CI

**Table 2** Studies Reporting the Diagnostic Yield and Performance of Robotic Bronchoscopy in Pulmonary Lesions

Study	Lesions (N)	Diagnostic Yield (DY)	Size mm (Diameter/Range)	Bronchus Sign	Pneumothorax/Intervention	Prevalence of Malignancy	Comment
<b>Ion Endoluminal System</b>							
Fielding 2019 <sup>45</sup>	29	88%	14.8 (10–26.4)	58.6%	0%/0%	88%	Feasibility Study, Successful navigation 96.6%
Benn 2021 <sup>46</sup>	52	86%	21.9 (7–60%)	46%	3.8%/1.4%	65%	Prospective, Successful navigation 85%, 15% repositioning with CBCT
PRECISE Study 2021 <sup>47</sup>	69	88%	17 (10–30)	25%	1.4%/0%	73%	Prospective multicenter cohort. 12 nonmalignant diagnoses
Reisenauer 2021 <sup>35</sup>	270	–	18.2 (10–30)	–	3.3%/0.4%	–	R-EBUS visualization in 89%. Mean 7th generation airways

(Continued)

Table 2 (Continued).

Study	Lesions (N)	Diagnostic Yield (DY)	Size mm (Diameter/Range)	Bronchus Sign	Pneumothorax/Intervention	Prevalence of Malignancy	Comment
Reisenauer 2021 <sup>48</sup>	30	93.3%	17.5 (10–30)	40%	0%/0%	73.3%	Prospective, feasibility cohort R-EBUS and 3D fluoroscopy (CIOS).
Bajwa 2021 <sup>49</sup>	76	92%	17 (0.6–70)	-	-	59%	R-EBUS 100%, 91% of inflammatory lesions resolved
Kalchiem-Dekel 2021 <sup>50</sup>	131	81.7%	18 (13–27)	62.9%	1.5%/1.5%	56.6%	Fluoroscopy: 2D 80%, 3D 20%, R-EBUS 85%
Oberg 2022 <sup>51</sup>	120	90%	22 (8–34.3)	48.3%	5.4%/2.7%	46.7%	Retrospective. R-EBUS + 2D fluoroscopy. Cryobiopsy with 1.1 mm probe.
Styrvoký 2022 <sup>52</sup>	209	91.4%	22.6 (7–73)	-	1%/0.5%	64.1%	Retrospective. R-EBUS and CBCT in 100%,
Low 2022 <sup>26</sup>	143	77%	17 (12–27)	40%	1.5%/1.5%	54.5%	Retrospective comparative cohort vs Digital tomosynthesis ENB. 100% R-EBUS and 2D fluoroscopy
<b>Monarch System</b>							
Rojas Solano 2018 <sup>53</sup>	15	-	26 (10–63)	100%	0%/0%	60%	Feasibility study, successful biopsy in 93%
Chaddha 2019 <sup>44</sup>	165	69.1%	25 (10–40)	63.5%	3.6%/2.4%	63.5%	Retrospective. R-EBUS signal and bronchus sign predicted success, no CBCT.
BENEFIT 2020 <sup>54</sup>	54	74.1%	23 (10–50)	59.3%	3.7%/1.9%	82.5%	Prospective multicentric feasibility. R-EBUS + 2D fluoroscopy. 96.2% localization rate.
Ekeke 2021 <sup>37</sup>	25	96%	20.5 (8–69)	84%	-	76%	Retrospective.
Agrawal 2022 <sup>55</sup>	124	77%	20.5 (13–30)	75%	1.6%	61%	Retrospective, 2D fluoroscopy, R-EBUS in 82%. Accuracy after 12-month follow-up overall sensitivity for malignancy 69%, specificity 100%
Cumbo-Nacheli 2022 <sup>56</sup>	20	86% Sensitivity	22 (15–29)	50%	-	75%	Retrospective. CBCT + R-EBUS. Pre-navigation CBCT, 100% navigation success.
Khan 2023 <sup>41</sup>	264	Index: 85.2% 12 months: 79.4%	19.3 (3.2–72.5)	30%	5.7%/3.8%	58%	Retrospective. R-EBUS in 93.9%, CBCT in 3.4%

2.4–22.9  $p < 0.001$ ), the DY was only 26.9% when no signal was encountered.<sup>44</sup> This should be contrasted against other studies where only 25% to 48% of patients had a demonstrable bronchus sign present, despite similar DY outcomes (these studies have used the Ion platform).<sup>47,48,51</sup> Other confirmation techniques or sampling instruments could optimize success rates despite the absence of a bronchus sign. Agrawal encountered a similar pattern with an 85%, 84%, and 38% DY of robotic biopsies for concentric, eccentric, and absent R-EBUS signals ( $p < 0.001$  for the trend), in this study after 12 months of follow-up and multivariate analysis, the R-EBUS signal and lesion size were the most important predictors of accuracy (87% in lesions  $> 20$  mm vs 82% in lesions  $< 20$  mm).<sup>55</sup>

As mentioned, a crucial parameter in current diagnostic success is the possibility of performing molecular analyses of the samples. In a retrospective study of 104 primary lung cancers and 24 metastatic lesions biopsied with ssRAB, Connolly found that 84% (108) of the samples were adequate for molecular testing. PCR-based testing for KRAS and EGFR mutations in adenocarcinomas was successful in 94% of the cases, and hybrid capture next-generation sequencing of 505 cancer genes was successful in 96% of the attempted samples. In addition, PD-L1 immunohistochemistry was successful in 91% of the attempted samples. Adequacy on ROSE was a predictor of greater tumor cellularity and success in molecular analyses (there was no difference with the use of larger bore 19-Gauge TBNA needles or more needle passes).<sup>57</sup> This is similar to the NAVIGATE ENB trial findings and EBUS TBNA data.

An essential clinical dilemma is assessing the value of a nonmalignant pathology result after RAB. This question requires longitudinal follow-up to ascertain the reliability of nonmalignant diagnoses, in addition to other confirmatory diagnostic techniques and evaluation of the clinical progression of the patient. In the study by Reisenauer, 32% of the ssRAB diagnoses were nonmalignant, with a false negative rate of 12%.<sup>58</sup> A second study that followed patients for 12 months found a 32% incidence of benign and 30% of nondiagnostic findings. This study had no false positives, with specificities and positive predictive values of 100%. Of 59 lesions negative for malignancy upon RAB sampling, 29 were later found to have malignant pathology upon follow-up (49% false negative rate).<sup>55</sup> Khan followed 264 patients after Monarch RAB, with 43% malignant, 41% benign (including specific: granulomas and infection, and non-specific: inflammation, organizing pneumonia, interstitial disease, etc.), and 15% non-diagnostic (normal tissue, atypical cells) results. The initial DY was 85%. After 12 months, benign nonspecific diagnoses had a false negative rate of 26%, with at least 17% (14/78) receiving a subsequent malignant diagnosis or radiographic progression. Non-diagnostic cases had a false negative rate of 43% (14/39). The final 12-month DY was 79% and varied when different definitions were used.<sup>41</sup>

In general, positive RAB results for malignancy are highly reliable. Unfortunately, false negatives are not uncommon and have been reported between 11–49%. Therefore, the decision to proceed with additional sampling methods and/or longitudinal follow-up after a negative or non-malignant RAB result should be based on patient characteristics, pretest probability, and multidisciplinary discussion.

Only one study has directly compared the performance of ssRAB vs CT-TTB. This retrospective study included 225 lesions and analyzed the diagnostic accuracy and sensitivity for malignancy at 12 months. Radial EBUS, CBCT, and ROSE were utilized universally. Sensitivities and NPV for detecting cancer of ssRAB and CT-TTB were similar (82.1% vs 88.5%,  $p = 0.674$  and 71.4 vs 62.9%,  $p = 0.17$ ). No false positives were encountered, yielding a specificity of 100% for both techniques. As discussed above, one of the most important clinical factors to consider is the likelihood of false negative results and the credibility of a nonmalignant result; in this study, the incidence of false negatives was similar in the two groups (12.3% vs 11.6%), with a true negative incidence of 30% for the ssRAB and 19.6% for the CCTB group. The incidence of complications was significantly higher in the CT-TTB group (17% vs 4.4%), with a pneumothorax rate of 16% vs 3% in the ssRAB group (OR 5.2). This study also highlights the advantageous possibility of performing only one procedure, including C-EBUS nodal staging at the time of RAB, as 37.5% of patients who underwent CT-TTB required a subsequent bronchoscopy with C-EBUS for staging.<sup>58</sup>

An updated meta-analysis including 16,389 PPL from 126 studies, of which six involved RAB (483 PPL), reported an overall DY of 77.6% (95% CI 70.4–84.8%). There was no significant difference when compared with R-EBUS, ENB with or without R-EBUS, VB, ultrathin or thin bronchoscopy with or without R-EBUS and/or virtual bronchoscopy. The pooled DY for all guided bronchoscopic procedures was 69.2%.<sup>24</sup> There was no statistically significant difference in the DY of bronchoscopic procedures before and after 2012.<sup>23</sup> The risks of selection bias, heterogeneity of studies, and lesion characteristics are also highlighted in these analyses. The largest and most recent meta-analysis, including 10,682 nodules

in 95 studies using navigational techniques, found a DY of 70.9%. RAB was utilized in 558 patients, with a yield of 76.5 (95% CI 60.4–87.4%).<sup>59</sup> Most importantly, the use of RAB, CBCT, or digital tomosynthesis (DT) guided EMN (discussed later) had a significantly higher DY than EMN alone and VB (77.5% vs 68.8%, respectively,  $p < 0.001$ ). When the newly proposed definitions were explored, the immediate/strict DY of all navigational techniques (based solely on results from the index procedure) was 68.6% for nodules  $> 20$  mm and 66.7% for smaller PPL when the intermediate definition was utilized at 12 months of follow up, the yields were 72.1% and 69.7% respectively. Although unable to make comparisons for significance, RAB and CBCT achieved the highest DY.<sup>42,59</sup> This meta-analysis highlights the clinical impact of improving the overall diagnostic performance when techniques such as robotic navigation or confirmation imaging (including its combination with other methods) are utilized.

## Biopsy Tools

Our knowledge of tool performance in PPL biopsy originates primarily from non-RAB studies. However, newer evidence from RAB studies is arising. In the NAVIGATE study, additional tools were utilized, such as the superDimension triple needle cytology brush in 303 cases, the GenCut core biopsy system (Medtronic, Minneapolis, MN) in 214 cases, and needle tipped cytology brushes in 241 patients, with 71% of the cases requiring at least three biopsy tools.<sup>22</sup> A subsequent analysis encountered that the use of multiple tools (6 instruments, including the above) had a higher DY for malignancy (86.8%) when compared to a restricted number of tools (biopsy forceps, standard cytology brush, and BAL) without increasing complications. The tools that contributed with the highest true positive rates were the biopsy forceps (86.9%) and aspirating needle (86.6%).<sup>60</sup> In a study at our institution utilizing the Ion ssRAB platform, concordance between ROSE and final histopathology was similar when needle and cold forceps were compared (89% for needle, 85% for forceps, and 92% overall).<sup>61</sup>

The use of parenchymal cryo-biopsies has demonstrated value in the diagnosis of interstitial and diffuse parenchymal lung diseases. With the development of a smaller flexible 1.1 mm cryoprobe (Erbe, Tuebingen, Germany), distal cryo-biopsies through  $> 1.2$  mm working channels are possible, with the potential of obtaining a radial sample devoid of crush artifact as opposed to forceps samples. Oberg reported a retrospective analysis of 120 peripheral nodules sampled with this probe utilizing ssRAB and R-EBUS guidance. The DY was 90%, and 18% of the diagnoses were made exclusively from the cryo-biopsy sample, with all cryo-biopsy samples demonstrating larger size, fewer artifacts, and sufficient material for molecular analysis.<sup>51</sup> The first prospective study is currently underway at the Mayo Clinic utilizing this mini-cryoprobe with the Ion ssRAB platform. (ROBOCOP study, NCT05399082).

## Confirmatory Techniques and Ancillary Imaging

The diagnostic success obtained from CT-TTB stems from the ability to reach the lesion with a straight pathway independent of airway anatomy and visualizing the target lesion and needle position during the procedure in real-time, allowing for confirmation of successful TIL. In RAB, it is ideal to have real-time confirmatory tools to demonstrate a TIL position, followed by the use of adequate tissue acquisition instruments (Figure 6).<sup>31</sup>

As planning and navigation rely almost exclusively on CT imaging, one of the most important concepts pertaining to confirmatory imaging and accuracy is the concept of “CT to body divergence”, by which the predominantly end-inspiratory and rapidly acquired helical images obtained in a high-resolution CT scanner can differ substantially from the situation of the patient in the procedural table.<sup>62</sup> Multiple factors can affect the actual position of the target lesions during the procedure: respiratory motion, positive pressure ventilation, and, more importantly, the acute development of atelectasis. In the I-LOCATE study, after a mean anesthesia time of only 33 minutes, 89% of the patients developed atelectasis in at least one segment. Up to 58% in 5 segments, with the superior, lateral, and posterior segments of the lower lobes being affected most commonly; this makes approaching lesions in these dependent areas more difficult, as pre-planned pathways and presumed lesion position would differ substantially from the pre-procedural CT.<sup>63</sup> Optimization of breath hold maneuvers by utilizing the pressure-limiting valve with adequate preoxygenation is important, the use of post-intubation recruitment maneuvers, and PEEP levels of 10–12 cmH<sub>2</sub>O, and occasionally higher for the lower lobes (commonly 15 cmH<sub>2</sub>O), as well as adequate timing of end-inspiratory breath holds during intraprocedural imaging are anesthetic techniques that can help reduce atelectasis-associated CT to body divergence.<sup>64</sup> The VESPA trial used a postintubation recruitment maneuver consisting of 10 breaths at a pressure control of 40 cmH<sub>2</sub>O with a PEEP



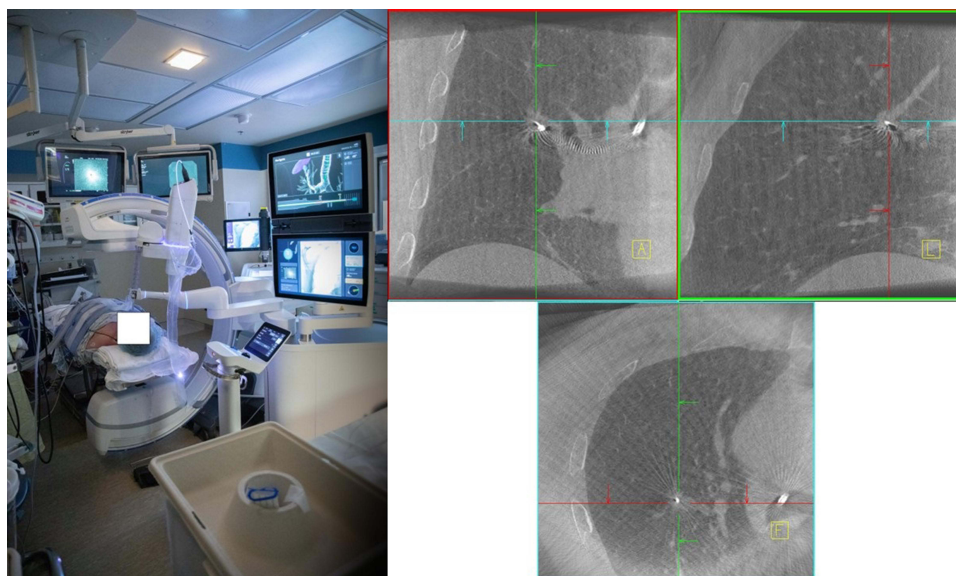


**Figure 6** Left: Room setup including the Ion ssRAB and the CIOS 3D-Spin Mobile CBCT (Siemens Healthineers, Malvern, PA). Right: CBCT images demonstrating a tool-in-lesion needle position (Courtesy of Dr. David Midthun. Mayo Clinic, Rochester, MN).

of 20cmH<sub>2</sub>O, PEEP was maintained at 8–10cmH<sub>2</sub>O, tidal volumes 6–8mL/Kg, and the FiO<sub>2</sub> was titrated to <100%; this strategy, compared with zero PEEP and 100% FiO<sub>2</sub> reduced the incidence of atelectasis on R-EBUS and CT from 84.2% to 28.9% ( $p < 0.0001$ ).<sup>39,64</sup> Using the lowest tolerated FiO<sub>2</sub> could theoretically reduce the incidence of resorption atelectasis.

Another crucial resource in addressing CT-to-body divergence is the use of confirmatory imaging. Intraprocedural tomographic imaging can corroborate a TIL position when attempting biopsies and aid in guiding instruments to the target. CBCT creates a 360° view by rotating a C-arm 180° plus the beam width, emitting cones of X-rays resulting in a series of 2D images, which are later reconstructed into a 3D series that can be reformatted into coronal, sagittal, axial, and volumetric images to locate and redirect the position of the target and the bronchoscopic/biopsy instruments. It differs from diagnostic CT, in which a helical source emits a thin fan beam X-ray array; CBCT cannot be used for diagnostics as there is reduced contrast, and the longer acquisition time produces more frequent motion artifacts but can generate a reconstruction significantly faster than DT.<sup>40</sup>

DT is a form of augmented fluoroscopy that utilizes limited exposure 2D fluoroscopic images with a limited angle of acquisition to yield images similar to conventional CT with a smaller area-focused field of view without requiring a complete 360° rotation, allowing for visualization and preprocedural location of fluoroscopically occult lesions; it has been used principally in combination with ENB, improving its performance. Recently, the use of tomosynthesis-augmented fluoroscopy using a conventional C-arm that can register the position of the nodule in real time and fuse the navigational images with the preprocedural CT (Illumisite, Medtronic, Minneapolis, MN) has allowed for real-time location of the nodule and bronchoscopic instruments and tracking of the position of the bronchoscope in the tomographic images.<sup>65</sup> In initial studies, this has improved the DY of ENB; its use with RAB is under investigation.<sup>66,67</sup> The RELIANT trial aims to compare the DY of the Illumisite with the ssRAB Ion Platform (NCT05705544). The TILT+™ Technology of the Galaxy system was discussed above.

In 2022, the FDA approved the integration of the Ion platform with the CIOS 3D-Spin Mobile CBCT (Siemens-Healthineers, Malvern, PA); this allows for review of CBCT images in the robotic console, with the possibility for re-registering target and instrument positions for renavigation, further reducing divergence.<sup>68</sup> Several studies have variably utilized axial reconstruction techniques in addition to conventional fluoroscopy with both RAB platforms (Table 2).<sup>52,56,68</sup> Benn et al encountered that in at least 15% of the cases, the CBCT image prompted changes in catheter position to target the lesion adequately.<sup>46</sup>

CT to body divergence was common in a pilot study at our institution utilizing the Ion/CIOS combination. Defined as >10 mm separation between the target location on the preprocedural CT and its location on CBCT, divergence was present in 60% of the

cases, with a median separation in the upper lobes of 10mm and 21mm in the lower lobes. Intraprocedural CBCT-guided adjustments of the robotic catheter allowed for a TIL success rate of 96.7% in 30 nodules with an average size of 17mm. The lower lobes had a divergence incidence of up to 82%, highlighting the importance of an intraprocedural imaging strategy to corroborate target and instrument position in real-time.<sup>48</sup> DT-based studies have shown comparable results, with mean divergences of 7–13 mm in the upper lobes and 14–16 mm in the lower lobes.<sup>66,67</sup> A new artificial intelligence-based augmented fluoroscopy platform able to assist with intra-procedural localization of the target and pathway generation (LungVision, Body Vision Medical, Ramat Ha Sharon, Israel) allows for real-time visualization of the lesion during the biopsy, creating an electronically highlighted target;<sup>65</sup> it increased the DY of a non ENB flexible bronchoscopic procedure up to 78.4% and measured a lower CT to body divergence distance than intraprocedural CBCT (5.9 vs 14.5 mm).<sup>69</sup> This system was recently utilized in patients undergoing ENB-RAB with a DY of 91%.<sup>70</sup> Augmented fluoroscopy features are currently being integrated into CBCT systems (Figure 7), including 3D fluoroscopy, allowing for improved real-time redirection of the instruments with >90% success rates.<sup>48,71</sup>

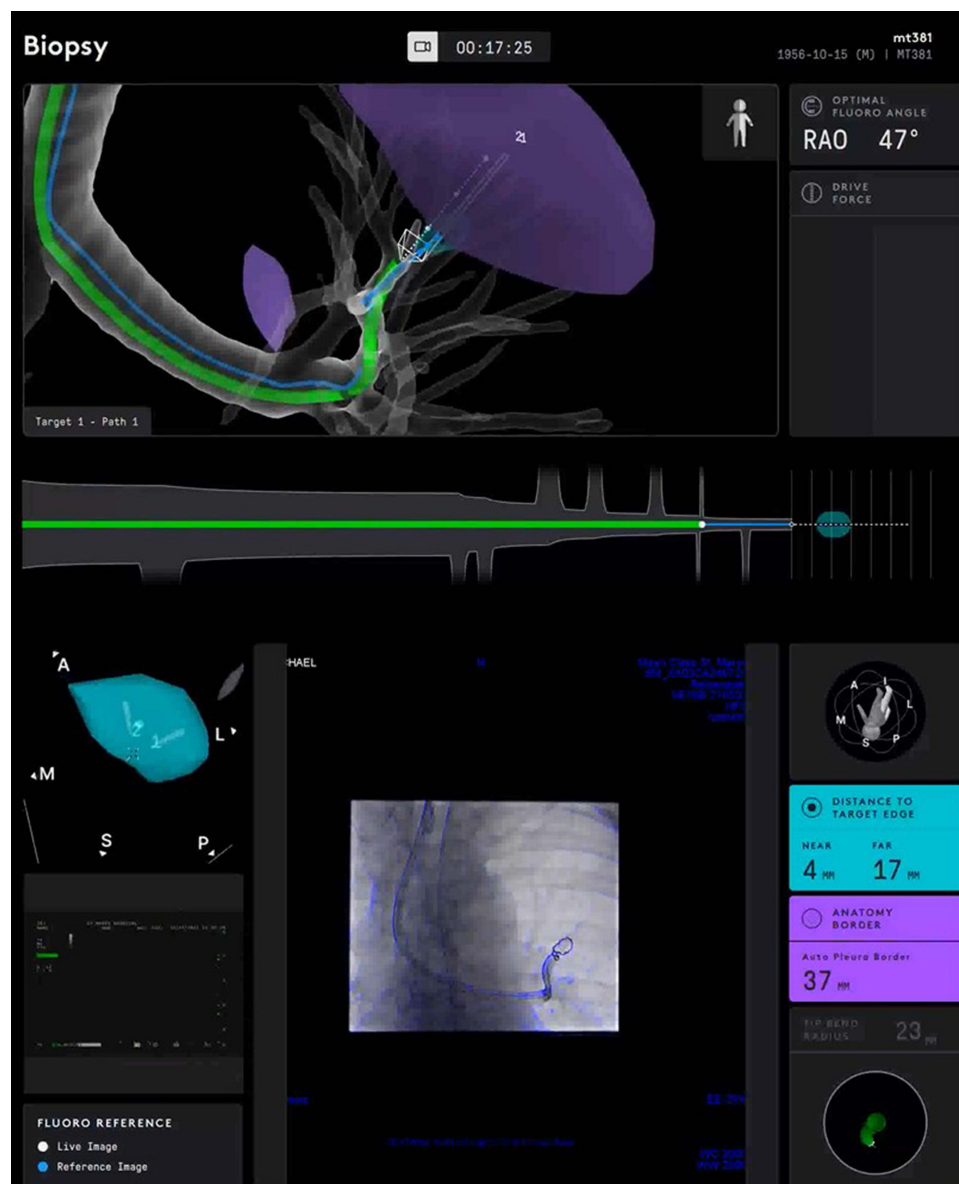


**Figure 7** Ion – CIOs CBCT integration demonstrating an augmented fluoroscopy live overlay of the catheter and the target lesion (automatic pleural border distance and tip Bend radius are displayed).

The role of ROSE has been evaluated in other contexts, allowing for fewer biopsy attempts without impacting overall procedural success. Specifically in RAB, in our institution, Vu et al found a concordance of 92% between ROSE and final pathology results in 110 ssRABs for PPL when combining all sampling instruments regardless of lesion size; only 9 cases were discordant. ROSE results were malignant in 70% of the cases and benign in 4%; importantly, non-diagnostic results were present in 26% of lesions by ROSE and pathology; upon follow-up, only a third of these resulted to be malignant, and 48% remained under observation without a malignant diagnosis.<sup>61</sup> In contrast, Aggarwal found that adequate ROSE specimens were obtained in 56% of the cases, with a concordance of 69% for those with a definitive malignant diagnosis.<sup>55</sup> This illustrates the ample variability in ROSE correlation with histopathology results and highlights its primary value in evaluating specimen adequacy.

## Complications in RAB

The most common clinically significant complication of RAB is iatrogenic pneumothorax; Table 2 summarizes the rate of pneumothoraces and intervention requirements. In the largest study with 270 PPL, the pneumothorax rate was 3.3%, and only one patient (0.4%) required a drain.<sup>35</sup> These rates are significantly lower than those associated with CT-TTNB. The position of the target lesion with respect to the pleural margins is a significant risk factor; both platforms have specific indicators that estimate the distance of the robotic catheter to the closest pleural surface.

Airway and parenchymal bleeding can rarely occur in RAB; in the mentioned study, 0.8% of the patients had bleeding of the airway that stopped within 5 minutes of tamponade, and no patient required additional hemostatic therapies.<sup>35</sup> In another study, with 24% of patients taking aspirin and 3% having pulmonary hypertension, significant bleeding was encountered only in 2.4% of the cases, and none required transfusions, endobronchial blockers, or other advanced therapies.<sup>44</sup> Some studies have not encountered any significant bleeding.<sup>54</sup> These findings suggest that bleeding with RAB is significantly less common and severe than in CT-TTB, being inconsequential in most cases. Derived from standard definitions of bleeding after transbronchial biopsy based on the duration of bleeding and the impact of required maneuvers,<sup>72</sup> efforts at preventing and optimizing the approach to bleeding have been made. Utilizing this grading system, an overall bleeding rate of 3.2% (4 patients) with only one patient having grade 2 bleeding was reported in a study of 95 PPL.<sup>55</sup> Optimization of hemostasis with potentially higher platelet thresholds (>50,000), the use of viscoelastic monitoring techniques, as well as strategies such as the use of parallel flexible bronchoscopy with the potential for rapid endobronchial occlusion have been proposed for high-risk cases and warrant further investigation.<sup>73,74</sup> Combination of studies and databases will be required to develop tools to predict bleeding risk due to its low incidence.

Al-ghoula et al performed a search in the FDA's MAUDE (Manufacturer and User Facility Device Experience) database for both platforms since their approval; a total of 513 incidents have been reported, pneumothorax being the most common (comprising 66.8% of all reported complications) followed by bleeding (10%). Only 12 deaths have been reported worldwide during or immediately following robotic bronchoscopy, five associated with pneumothorax. Forty-eight technical problems have been reported in this database, most commonly detachment or disconnection; unintended catheter movement has been reported in 8 cases.<sup>75</sup> A large study with a target population of 1200 is underway to evaluate the incidence of severe and intervention-warranting procedural complications using the Monarch platform (TARGET study NCT04182815).

## Therapeutic RAB Applications

RAB can deliver fiducial markers for radiotherapy with imaging confirmation and lower risk than other techniques. Special dyes such as Indocyanine green (ICG) injected after bronchoscopic localization confirmation allow for easier and more reliable lesion localization during thoroscopic resection procedures by utilizing near-infrared fluorescence imaging.<sup>76</sup> The ongoing REPLACING study aims at evaluating the feasibility of ICG injection into PPL using the Ion platform with CBCT (NCT04987281). This could have future impacts in better guidance for more conservative resections at a time when sub-lobar resections could be reconsidered and have shown comparable outcomes in adequately selected early lesions (Stage IA).<sup>77</sup> There has been a proposed "one-stop" approach, in which during a single anesthetic procedure, the patient undergoes a diagnostic RAB with ICG marking and EBUS staging, followed by a thoroscopic (frequently robotic) resection if appropriate.<sup>78</sup>

Multiple ablative therapies have been proposed for early-stage NSCLC, initially delivered via the transthoracic route; they have been recently employed endobronchially, including cryoablation, radiofrequency ablation, and microwave ablation (MWA).<sup>79</sup> These have been studied with ENB with promising results, including high success and low

progression rates;<sup>80</sup> RAB has the additional advantages of stabilization and confirmation of accurate delivery of therapy when combined with imaging techniques, and the potential for fewer complications, the main disadvantage being the lack of pathologic confirmation before treatment.<sup>81</sup> The POWER (Prospective Transbronchial Microwave + Robotic-Assisted Bronchoscopy) study is currently recruiting patients to assess the ablative efficacy of utilizing the Monarch platform with CBCT to deliver the NEUWAVE FLEX MWA system (NeuWave Medical, Madison, WI) to oligometastatic PPL located in the outer 2/3 of the thorax with >1 cm separation from the pleural surface (NCT05299606).

Pulsed electrical field therapy through a peripheral TBNA needle (PeriView Flex, Olympus, Center Valley, PA) has been undertaken trans-bronchoscopically in the INCITE ES trial (NCT04732520), producing tumor cell death with preservation of the surrounding tissue and potential stimulation of a more immunogenic response, based on a higher number of tertiary lymphoid structure formation within the tumors,<sup>82</sup> leading to the FDA 510(K) clearance of the Aliya system (Galvanize Therapeutics, San Carlos, CA).

Endobronchial delivery of chemotherapy and intratumoral therapies to PPL is being explored after initial efforts injecting agents to lesions in the proximal airways and lymphadenopathies using C-EBUS were completed. Transbronchial injections of standard cytotoxic agents such as cisplatin to early-stage lesions are being employed (NCT04809103).<sup>83</sup> Furthermore, therapies such as immunotherapy, oncolytic viruses, and gene therapies are being considered when a reliable endobronchial tumor localization can be achieved, such as that offered by RAB.<sup>84</sup>

## Conclusion

RAB results from a long trajectory of innovation in advanced and navigational bronchoscopy. With the changing epidemiology of lung cancer, prompted by more aggressive detection and treatment strategies, tools that provide precise tissue diagnosis in earlier and smaller lesions are a growing need. RAB allows for a combination of multiple technologies (EBUS, confirmatory imaging, and ROSE) to improve precision, achieving variable DY and high specificities contingent on the lesion and patient factors. Future developments in RAB and new combinations with other techniques are expected to improve its performance and expand its field of application with diagnostic and therapeutic purposes, likely translating into improvements in patient outcomes and satisfaction.

## Funding

The authors received no financial support for this article's research, authorship, and publication.

## Disclosure

Dr Janani Reisenauer reports grants from Intuitive Surgical outside the submitted work. The authors report no other conflicts of interest in this work.

## References

1. Thai AA, Solomon BJ, Sequist LV, Gainor JF, Heist RS. Lung cancer. *Lancet*. 2021;398(10299):535–554. doi:10.1016/s0140-6736(21)00312-3
2. Siegel RL, Miller KD, Fuchs HE, Jemal A. Cancer statistics, 2022. *Cancer J Clin*. 2022;72(1):7–33. doi:10.3322/caac.21708
3. Group USCSW. U.S. Cancer Statistics Data Visualizations Tool, based on 2021 submission data (1999–2019). U.S. Department of Health and Human Services, Centers for Disease Control and Prevention and National Cancer Institute; 2021.
4. Howlader N, Forjaz G, Mooradian MJ, et al. The effect of advances in lung-cancer treatment on population mortality. *N Engl J Med*. 2020;383(7):640–649. doi:10.1056/nejmoa1916623
5. Oken MM, Hocking WG, Kvale PA, et al. Screening by chest radiograph and lung cancer mortality. *JAMA*. 2011;306(17):1865. doi:10.1001/jama.2011.1591
6. Team TNLSTR. Reduced lung-cancer mortality with low-dose computed tomographic screening. *N Engl J Med*. 2011;365(5):395–409. doi:10.1056/nejmoa1102873
7. De Koning HJ, Van Der Aalst CM, De Jong PA, et al. Reduced lung-cancer mortality with volume CT screening in a randomized trial. *N Engl J Med*. 2020;382(6):503–513. doi:10.1056/nejmoa1911793
8. Landy R, Young CD, Skarzynski M, et al. Using prediction models to reduce persistent racial and ethnic disparities in the draft 2020 USPSTF lung cancer screening guidelines. *JNCI*. 2021;113(11):1590–1594. doi:10.1093/jnci/djaa211
9. D'Angelo SP, Janjigian YY, Ahye N, et al. Distinct clinical course of EGFR -mutant resected lung cancers: results of testing of 1118 surgical specimens and effects of adjuvant gefitinib and erlotinib. *J Thorac Oncol*. 2012;7(12):1815–1822. doi:10.1097/jto.0b013e31826bb7b2
10. Kris MG, Johnson BE, Berry LD, et al. Using multiplexed assays of oncogenic drivers in lung cancers to select targeted drugs. *JAMA*. 2014;311(19):1998. doi:10.1001/jama.2014.3741



11. Lindeman NI, Cagle PT, Aisner DL, et al. Updated molecular testing guideline for the selection of lung cancer patients for treatment with targeted tyrosine kinase inhibitors. *J Mol Diagn*. 2018;20(2):129–159. doi:10.1016/j.jmoldx.2017.11.004
12. Labarca G, Folch E, Jantz M, Mehta HJ, Majid A, Fernandez-Bussy S. Adequacy of samples obtained by endobronchial ultrasound with transbronchial needle aspiration for molecular analysis in patients with non-small cell lung cancer. Systematic review and meta-analysis. *Ann Am Thorac Soc*. 2018;15(10):1205–1216. doi:10.1513/AnnalsATS.201801-045OC
13. Forde PM, Spicer J, Lu S, et al. Neoadjuvant nivolumab plus chemotherapy in resectable lung cancer. *N Engl J Med*. 2022;386(21):1973–1985. doi:10.1056/nejmoa2202170
14. Wakelee H, Liberman M, Kato T, et al. Perioperative pembrolizumab for early-stage non-small-cell lung cancer. *N Engl J Med*. 2023. doi:10.1056/nejmoa2302983
15. Gould MK, Donington J, Lynch WR, et al. Evaluation of individuals with pulmonary nodules: when is it lung cancer? *Chest*. 2013;143(5):e93S–e120S. doi:10.1378/chest.12-2351
16. Wiener RS, Schwartz LM, Woloshin S, Welch HG. Population-based risk for complications after transthoracic needle lung biopsy of a pulmonary nodule: an analysis of discharge records. *Ann Intern Med*. 2011;155(3):137. doi:10.7326/0003-4819-155-3-201108020-00003
17. Huo YR, Chan MV, Habib AR, Lui I, Ridley L. Pneumothorax rates in CT-Guided lung biopsies: a comprehensive systematic review and meta-analysis of risk factors. *Br J Radiol*. 2020;93(1108):20190866. doi:10.1259/bjr.20190866
18. Rivera MP, Mehta AC, Wahidi MM. Establishing the diagnosis of lung cancer. *Chest*. 2013;143(5):e142S–e165S. doi:10.1378/chest.12-2353
19. Tanner NT, Yarmus L, Chen A, et al. Standard bronchoscopy with fluoroscopy vs thin bronchoscopy and radial endobronchial ultrasound for biopsy of pulmonary lesions. *Chest*. 2018;154(5):1035–1043. doi:10.1016/j.chest.2018.08.1026
20. Mehta AC, Hood KL, Schwarz Y, Solomon SB. The evolutionary history of electromagnetic navigation bronchoscopy: state of the art. *Chest*. 2018;154(4):935–947. doi:10.1016/j.chest.2018.04.029
21. Lachkar S, Perrot L, Gervereau D, et al. Radial-EBUS and virtual bronchoscopy planner for peripheral lung cancer diagnosis: how it became the first-line endoscopic procedure. *Thoracic Cancer*. 2022;13(20):2854–2860. doi:10.1111/1759-7714.14629
22. Folch EE, Bowling MR, Pritchett MA, et al. NAVIGATE 24-month results: electromagnetic navigation bronchoscopy for pulmonary lesions at 37 centers in Europe and the United States. *J Thorac Oncol*. 2022;17(4):519–531. doi:10.1016/j.jtho.2021.12.008
23. Wang Memoli JS, Nietert PJ, Silvestri GA. Meta-analysis of guided bronchoscopy for the evaluation of the pulmonary nodule. *Chest*. 2012;142(2):385–393. doi:10.1378/chest.11-1764
24. Nadig TR, Thomas N, Nietert PJ, et al. Guided bronchoscopy for the evaluation of pulmonary lesions: an updated meta-analysis. *Chest*. 2023;163(6):1589–1598. doi:10.1016/j.chest.2022.12.044
25. Folch EE, Labarca G, Ospina-Delgado D, et al. Sensitivity and safety of electromagnetic navigation bronchoscopy for lung cancer diagnosis: systematic review and meta-analysis. *Chest*. 2020;158(4):1753–1769. doi:10.1016/j.chest.2020.05.534
26. Low SW, Lentz RJ, Chen H, et al. Shape-sensing robotic-assisted bronchoscopy vs digital tomosynthesis-corrected electromagnetic navigation bronchoscopy: a comparative cohort study of diagnostic performance. *Chest*. 2023;163(4):977–984. doi:10.1016/j.chest.2022.10.019
27. U.S. Food and Drug Administration. 510(k) premarket notification - ion endoluminal system. Report K192367; 2022.
28. Duke JD, Reisenauer J. Review: technology and techniques for robotic-assisted bronchoscopy. *J Lung Health Dis*. 2022;6(1):1–5. doi:10.29245/2689-999x/2022/1.1179
29. Diddams MJ, Lee HJ. Robotic bronchoscopy: review of three systems. *Life*. 2023;13(2):354. doi:10.3390/life13020354
30. Ho E, Hedstrom G, Murgu S. Robotic bronchoscopy in diagnosing lung cancer—the evidence, tips and tricks: a clinical practice review. *Ann Transl Med*. 2023;1(1):1. doi:10.21037/atm-22-3078
31. Folch E, Mittal A, Oberg C. Robotic bronchoscopy and future directions of interventional pulmonology. *Curr Opin Pulm Med*. 2022;28(1):37–44. doi:10.1097/mcp.0000000000000849
32. Bhadra K, Rickman OB, Mahajan AK, Hogarth DK. “Tool-in-lesion” accuracy of galaxy system—A robotic electromagnetic navigation bronchoscopy with integrated tool-in-lesion-tomosynthesis technology: the MATCH Study. *J Bronchology Interv Pulmonol*. 2023. doi:10.1097/lbr.0000000000000923
33. Cho RJ, Keenan J, Murgu S. The feasibility of using the “vessel sign” for pre-procedural planning in navigation bronchoscopy for peripheral pulmonary lesion sampling: a dual-center retrospective study. *Am J Respir Crit Care Med*. 2023;207:A3670–A3670. doi:10.1164/ajrcm-conference.2022.205.1\_MeetingAbstracts.A3670
34. Ho E, Cho RJ, Keenan JC, Murgu S. The feasibility of using the “artery sign” for pre-procedural planning in navigational bronchoscopy for parenchymal pulmonary lesion sampling. *Diagnostics*. 2022;12(12):3059. doi:10.3390/diagnostics12123059
35. Reisenauer J, Simoff MJ, Pritchett MA, et al. Ion: technology and techniques for shape-sensing robotic-assisted bronchoscopy. *Ann Thorac Surg*. 2022;113(1):308–315. doi:10.1016/j.athoracsur.2021.06.086
36. Akulian JA, Molena D, Wahidi MM, et al. A direct comparative study of bronchoscopic navigation planning platforms for peripheral lung navigation: the ATLAS study. *J Bronchology Interv Pulmonol*. 2022;29(3):171–178. doi:10.1097/lbr.0000000000000806
37. Ekeke CN, Vercauteren M, Istvaniczdavkovic S, Semaan R, Dhupar R. Lung nodule evaluation using robotic-assisted bronchoscopy at a veteran’s affairs hospital. *J Clin Med*. 2021;10(16):3671. doi:10.3390/jcm10163671
38. McLoughlin KC, Bott MJ. Robotic bronchoscopy for the diagnosis of pulmonary lesions. *Thorac Surg Clin*. 2023;33(1):109–116. doi:10.1016/j.thorsurg.2022.08.008
39. Salahuddin M, Sarkiss M, Sagar AS, et al. Ventilatory strategy to prevent atelectasis during bronchoscopy under general anesthesia: a multicenter randomized controlled trial (ventilatory strategy to prevent atelectasis -VESPA- trial). *Chest*. 2022;162(6):1393–1401. doi:10.1016/j.chest.2022.06.045
40. Setser R, Chintalapani G, Bhadra K, Casal RF. Cone beam CT imaging for bronchoscopy: a technical review. *J Thorac Dis*. 2020;12(12):7416–7428. doi:10.21037/jtd-20-2382
41. Khan F, Seaman J, Hunter TD, et al. Diagnostic outcomes of robotic-assisted bronchoscopy for pulmonary lesions in a real-world multicenter community setting. *BMC Pulm Med*. 2023;23(1). doi:10.1186/s12890-023-02465-w
42. Vachani A, Maldonado F, Laxmanan B, Kalsekar I, Murgu S. The impact of alternative approaches to diagnostic yield calculation in studies of bronchoscopy. *Chest*. 2022;161(5):1426–1428. doi:10.1016/j.chest.2021.08.074



43. Yarmus L, Wahidi M, Lee H, et al. The PRECISION-1 study: a prospective single-blinded randomized comparative study of three guided bronchoscopic approaches for investigating pulmonary nodules. *Chest*. 2019;156(4):A2256–A2257. doi:10.1016/j.chest.2019.08.311
44. Chaddha U, Kovacs SP, Manley C, et al. Robot-assisted bronchoscopy for pulmonary lesion diagnosis: results from the initial multicenter experience. *BMC Pulm Med*. 2019;19(1):243. doi:10.1186/s12890-019-1010-8
45. Fielding DIK, Bashirzadeh F, Son JH, et al. First human use of a new robotic-assisted fiber optic sensing navigation system for small peripheral pulmonary nodules. *Respiration*. 2019;98(2):142–150. doi:10.1159/000498951
46. Benn BS, Romero AO, Lum M, Krishna G. Robotic-assisted navigation bronchoscopy as a paradigm shift in peripheral lung access. *Lung*. 2021;199(2):177–186. doi:10.1007/s00408-021-00421-1
47. Ost D, Pritchett M, Reisenauer J, et al. Prospective multicenter analysis of shape-sensing robotic-assisted bronchoscopy for the biopsy of pulmonary nodules: results from the PRECISE study. *Chest*. 2021;160(4):A2531–A2533. doi:10.1016/j.chest.2021.08.034
48. Reisenauer J, Duke JD, Kern R, Fernandez-Bussy S, Edell E. Combining shape-sensing robotic bronchoscopy with mobile three-dimensional imaging to verify tool-in-lesion and overcome divergence: a pilot study. *Mayo Clin Proc*. 2022;6(3):177–185. doi:10.1016/j.mayocpiqo.2022.02.004
49. Bajwa A, Bawek S, Bajwa S, Rathore A. 76 Consecutive Cases of Robotic-Assisted Navigational Bronchoscopy at a Single Center. *Am J Respir Crit Care Med*. 2021; 203: A4820. doi:10.1164/ajrccm-conference.2021.203.1\_MeetingAbstracts.A4820
50. Kalchiem-Dekel O, Connolly JG, Lin IH, et al. Shape-sensing robotic-assisted bronchoscopy in the diagnosis of pulmonary parenchymal lesions. *Chest*. 2022;161(2):572–582. doi:10.1016/j.chest.2021.07.2169
51. Oberg CL, Lau RP, Folch EE, et al. Novel robotic-assisted cryobiopsy for peripheral pulmonary lesions. *Lung*. 2022;200(6):737–745. doi:10.1007/s00408-022-00578-3
52. Styrvoky K, Schwalk A, Pham D, et al. Shape-sensing robotic-assisted bronchoscopy with concurrent use of radial endobronchial ultrasound and cone beam computed tomography in the evaluation of pulmonary lesions. *Lung*. 2022;200(6):755–761. doi:10.1007/s00408-022-00590-7
53. Rojas-Solano JR, Ugalde-Gamboa L, Machuzak M. Robotic bronchoscopy for diagnosis of suspected lung cancer: a feasibility study. *J Bronchology Interv Pulmonol*. 2018;25(3):168–175. doi:10.1097/lbr.0000000000000499
54. Chen AC, Pastis NJ, Mahajan AK, et al. Robotic bronchoscopy for peripheral pulmonary lesions. *Chest*. 2021;159(2):845–852. doi:10.1016/j.chest.2020.08.2047
55. Agrawal A, Ho E, Chaddha U, et al. Factors associated with diagnostic accuracy of robotic bronchoscopy with 12-month follow-up. *Ann Thorac Surg*. 2022 ;115(6): 1361–1368. doi:10.1016/j.athoracsur.2021.12.041
56. Cumbo-Nacheli G, Velagapudi RK, Enter M, Egan JPI, Conci D. Robotic-assisted bronchoscopy and cone-beam CT: a retrospective series. *J Bronchology Interv Pulmonol*. 2022;29(4):303–306. doi:10.1097/lbr.0000000000000860
57. Connolly JG, Kalchiem-Dekel O, Tan KS, et al. Feasibility of shape-sensing robotic-assisted bronchoscopy for biomarker identification in patients with thoracic malignancies. *J Thorac Cardiovasc Surg*. 2022. doi:10.1016/j.jtcvs.2022.10.059
58. Yu Lee-Mateus A, Reisenauer J, Garcia-Saucedo JC, et al. Robotic-assisted bronchoscopy versus CT-guided transthoracic biopsy for diagnosis of pulmonary nodules. *Respirology*. 2023;28(1):66–73. doi:10.1111/resp.14368
59. Kops SEP, Heus P, Korevaar DA, et al. Diagnostic yield and safety of navigation bronchoscopy: a systematic review and meta-analysis. *Lung Cancer*. 2023;180:107196. doi:10.1016/j.lungcan.2023.107196
60. Gildea TR, Folch EE, Khandhar SJ, et al. The impact of biopsy tool choice and rapid on-site evaluation on diagnostic accuracy for malignant lesions in the prospective: multicenter NAVIGATE study. *J Bronchology Interv Pulmonol*. 2021;28(3):174–183. doi:10.1097/lbr.0000000000000740
61. Vu LH, Yu Lee-Mateus A, Edell ES, et al. Accuracy of preliminary pathology for robotic bronchoscopic biopsy. *Ann Thorac Surg*. 2022. doi:10.1016/j.athoracsur.2022.11.022
62. Pritchett MA, Bhadra K, Calcutt M, Folch E. Virtual or reality: divergence between preprocedural computed tomography scans and lung anatomy during guided bronchoscopy. *J Thorac Dis*. 2020;12(4):1595–1611. doi:10.21037/jtd.2020.01.35
63. Sagar AS, Sabath BF, Eapen GA, et al. Incidence and location of atelectasis developed during bronchoscopy under general anesthesia: the I-LOCATE trial. *Chest*. 2020;158(6):2658–2666. doi:10.1016/j.chest.2020.05.565
64. Pritchett MA, Lau K, Skibo S, Phillips KA, Bhadra K. Anesthesia considerations to reduce motion and atelectasis during advanced guided bronchoscopy. *BMC Pulm Med*. 2021;21(1):1.
65. Ravikumar N, Ho E, Wagh A, Murgu S. Advanced imaging for robotic bronchoscopy: a review. *Diagnostics*. 2023;13(5):990. doi:10.3390/diagnostics13050990
66. Aboudara M, Roller L, Rickman O, et al. Improved diagnostic yield for lung nodules with digital tomosynthesis-corrected navigational bronchoscopy: initial experience with a novel adjunct. *Respirology*. 2020;25(2):206–213. doi:10.1111/resp.13609
67. Katsis J, Roller L, Aboudara M, et al. Diagnostic yield of digital tomosynthesis-assisted navigational bronchoscopy for indeterminate lung nodules. *J Bronchology Interv Pulmonol*. 2021;28(4):255–261. doi:10.1097/lbr.0000000000000766
68. Duke JD, Sanborn D, Reisenauer J. Enhancing nodule biopsy through technology integration. *Innovations*. 2023;15569845231153639. doi:10.1177/15569845231153639
69. Pritchett MA. Prospective analysis of a novel endobronchial augmented fluoroscopic navigation system for diagnosis of peripheral pulmonary lesions. *J Bronchology Interv Pulmonol*. 2021;28(2):107–115. doi:10.1097/lbr.0000000000000700
70. Hedstrom G, Wagh A. Combining real-time 3-D imaging and augmented fluoroscopy with robotic bronchoscopy for the diagnosis of peripheral lung nodules. *Chest*. 2022;162(4 Suppl):A2082. doi:10.1016/j.chest.2022.08.1720
71. Kalchiem-Dekel O, Fuentes P, Bott MJ, et al. Multiplanar 3D fluoroscopy redefines tool–lesion relationship during robotic-assisted bronchoscopy. *Respirology*. 2021;26(1):120–123. doi:10.1111/resp.13966
72. Folch EE, Mahajan AK, Oberg CL, et al. Standardized definitions of bleeding after transbronchial lung biopsy: a delphi consensus statement from the Nashville Working Group. *Chest*. 2020;158(1):393–400. doi:10.1016/j.chest.2020.01.036
73. Fernandez-Bussy S, Abia-Trujillo D, Majid A, et al. Management of significant airway bleeding during robotic assisted bronchoscopy: a tailored approach. *Respiration*. 2021;100(6):547–550. doi:10.1159/000514830
74. Fernandez-Bussy S, Abia-Trujillo D, Patel NM, et al. Precautionary strategy for high-risk airway bleeding cases during robotic-assisted bronchoscopy. *Respirol Case Rep*. 2021;9(7):1.

75. Al-ghoula F, Albitar H, Nelson D. *Exploring the Complications and Challenges of Robotic Bronchoscopy: Insights from MAUDE Database*. Mayo Clinic; 2023.
76. Cui F, Liu J, Du M, et al. Expert consensus on indocyanine green fluorescence imaging for thoracoscopic lung resection (the version 2022). *Transl Lung Cancer Res*. 2022;11(11):2318–2331. doi:10.21037/tlcr-22-810
77. Altorki N, Wang X, Kozono D, et al. Lobar or sublobar resection for peripheral stage IA non-small-cell lung cancer. *N Engl J Med*. 2023;388(6):489–498. doi:10.1056/nejmoa2212083
78. Chan JWY, Chang ATC, Yu PSY, Lau RWH, Ng CSH. Robotic assisted-bronchoscopy with cone-beam CT ICG dye marking for lung nodule localization: experience beyond USA. *Front Surg*. 2022;9. doi:10.3389/fsurg.2022.943531
79. Maxwell CM, Ng C, Fernando HC. Stereotactic body radiation therapy versus ablation versus surgery for early-stage lung cancer in high-risk patients. *Thorac Surg Clin*. 2023;33(2):179–187. doi:10.1016/j.thorsurg.2023.01.003
80. Siu ICH, Chan JWY, Manuel Ii TB, Ngai JCL, Lau RWH, Ng CSH. Bronchoscopic ablation of lung tumours: patient selection and technique. *J Vis Surg*. 2022;8:36. doi:10.21037/jovs-21-45
81. Chan JWY, Siu ICH, Chang ATC, et al. Transbronchial techniques for lung cancer treatment: where are we now? *Cancers*. 2023;15(4):1068. doi:10.3390/cancers15041068
82. Iding J, VanderLaan P, Jimenez M, et al. 702 Tertiary lymphoid structures (TLS) observed in non-small cell lung cancer (NSCLC) tumors treated with pulsed electric fields. *J Immunother Cancer*. 2022;10(Suppl 2):A733–A735. doi:10.1136/jitc-2022-SITC2022.0702
83. Ji Y, Luan S, Yang X, et al. Efficacy of bronchoscopic intratumoral injection of endostar and cisplatin in lung squamous cell carcinoma patients underwent conventional chemoradiotherapy. *Open Med*. 2023;18(1). doi:10.1515/med-2023-0640
84. Demaio A, Serman D. Bronchoscopic intratumoural therapies for non-small cell lung cancer. *Eur Respir Rev*. 2020;29(156):200028. doi:10.1183/16000617.0028-2020

## Pragmatic and Observational Research

Dovepress

### Publish your work in this journal

Pragmatic and Observational Research is an international, peer-reviewed, open access journal that publishes data from studies designed to reflect more closely medical interventions in real-world clinical practice compared with classical randomized controlled trials (RCTs). The manuscript management system is completely online and includes a very quick and fair peer-review system. Visit <http://www.dovepress.com/testimonials.php> to read real quotes from published authors.

Submit your manuscript here: <http://www.dovepress.com/pragmatic-and-observational-research-journal>